Article Beitr. Phys. Atmosph., November 1994, p. 341–351
0005-8173/94/04 0341–11 $ 3.00/0 Vol. 67, No. 4 341

Distribution of Trace Substances Inside and Outside of Clouds

by M. PREISS[1], R. MASER[1], H. FRANKE[1], W. JAESCHKE[1] and J. GRAF[2]

[1]Zentrum für Umweltforschung, J. W. Goethe-Universität, Georg-Voigt-Str. 14, 60325 Frankfurt am Main, Germany
[2]Institut für Physik der Atmosphäre, DLR Oberpfaffenhofen, 82330 Weßling, Germany

(Manuscript received April 18, 1994; accepted October 17, 1994)

Abstract

During the CLEOPATRA campaign 7 measuring flights have been conducted. The aim was a determination of trace constituents in and in the vicinity of clouds. For this purpose microphysical and chemical measurements were carried out and cloud water was collected. The trace gas concentrations of SO_2, H_2O_2, O_3, NO, NO_2 and NO_x were determined. Cloud water samples were analysed for S(IV), H_2O_2, pH, conductivity, Cl^-, NO_3^-, SO_4^{2-}, NH_4^+, Na^+, K^+, Ca^{2+} and Mg^{2+}. Furthermore cloud droplet size distribution, LWC, pressure, relative humidity and temperature were continuously measured. During the entire campaign low S(IV) concentrations have been measured. They ranged between 0.1–4 µmol/l. In contrast measured H_2O_2 concentrations and pH were relatively high. H_2O_2 concentrations raised up to 155 µmol/l and highest pH was 6.9. For the first time H_2O_2 and S(IV) concentrations of cloud water droplets were measured on-line on board of the aircraft. With the possibility of direct S(IV) analyses, the SO_2/S (IV) phase equilibrium has been examined.

Zusammenfassung

Spurenstoffverteilung innerhalb und außerhalb von Wolken

Im Rahmen des CLEOPATRA-Experiments wurden bei sieben Meßflügen im süddeutschen Raum zur Bestimmung der Spurenstoffverteilung innerhalb und außerhalb von Wolken chemische und mikrophysikalische Messungen durchgeführt sowie Wolkenwasserproben gesammelt. Dabei wurden die Spurengase SO_2, H_2O_2, O_3, NO, NO_2 und NO_x gemessen. Die gesammelten Wolkenwasserproben wurden auf die Komponenten S(IV), H_2O_2, pH, Leitfähigkeit, Cl^-, NO_3^-, SO_4^{2-}, NH_4^+, Na^+, K^+, Ca^{2+} and Mg^{2+} untersucht. Zur Erfassung der mikrophysikalischen Randbedingungen wurden das Tropfenspektrum, der LWC, der Druck, die relative Feuchte und die Temperatur aufgezeichnet. Die gemessenen Sulfitkonzentrationen waren im Meßzeitraum niedrig (0.1–4 µmol/l), während sowohl der pH-Wert als auch die H_2O_2-Konzentrationen außergewöhnlich hoch waren. Die pH-Werte erreichten Werte bis 6.9, Spitzenkonzentrationen von H_2O_2 lagen bei 155 µmol/l. S(IV) and H_2O_2 wurden erstmals on-line im Flugzeug analysiert und das SO_2/S(IV) Phasengleichgewicht untersucht.

1 Introduction

The chemical composition of clouds is of current interest because of the role of clouds in the transformation of trace atmospheric constituents and the production of atmospheric acidity. A key question is the extent to which clouds simply dissolve soluble aerosol and gases present in free cloud atmosphere or alternatively serve as a reaction medium. The gas scavenging of trace gases like SO_2 and their chemical reactions in the aqueous phase strongly influences the chemical composition of the cloud droplet and their pH.

The aim during the CLEOPATRA experiment was the investigation of the uptake of the gaseous SO_2 and H_2O_2 into the cloud and the chemical reactions which occur in the cloud droplet. Of special interest was the examination of the SO_2/S(IV) phase equilibrium. Previous field studies have shown that Henry's law equilibrium is not always fulfilled in

atmospheric samples of bulk cloud water. With the possibility to analyse S (IV) on-line on board of the aircraft and to differentiate between free S (IV) and carbonyl bounded S (IV) a re-study of the gas/liquid equilibrium was intended.

This report is a summary of measurements performed during seven flights in May and July 1992. Measurements include continuous in-situ monitoring of O_3, NO, NO_2, NO_x, SO_2 and H_2O_2. Additionally major ionic species (H^+, NH_4^+, Na^+, K^+, Ca^{2+}, Mg^{2+}, Cl^-, NO_3^- and SO_4^{2-}) were determined.

2 Experimental Description

2.1 Measuring Systems

Measurements were conducted with three aircraft: a Piper Navajo Chieftain, a DO-228 and a DO-128. In this paper results of measurements obtained with the first two aircraft are presented. The equipment of the aircraft is described in detail by Maser et al. (this issue) and in the TRACT Quality Assurance project plan (Mohnen et al., 1992). Therefore here only a brief overview will be presented. Standard meteorological instrumentation was installed on board of the aircraft (temperature, pressure, windspeed, LWC and relative humidity). For the registration of the cloud droplet size distribution a Knollenberg forward scattering probe (FSSP-100) has been used. Gasphase concentrations of O_3, NO, NO_2, NO_x, SO_2 and H_2O_2 were measured continuously on board of the aircraft. Cloud water samples were analysed immediately after sampling for S (IV) and H_2O_2 with a continuous flow chemiluminescence analyser (see Maser, this issue). Right after landing, the cloud water pH and conductivity has been determined. Major anions and cations have been analysed by ion chromatography.

2.2 Flight Pattern

For the measuring flights during the CLEOPATRA experiment three different flight pattern for different weather conditions have been chosen (Maser et al., this issue). For cumulus convection pattern C has been designed with fixed flight levels for each aircraft. The two aircraft had been separated only vertically by a distance of about 1000 m. Pattern A and B were chosen for stratiform clouds with flights in south-north respectively in east-west directions in three different heights. Additionally flights in single cumulus clouds have been conducted. In Figure 1, the flight pattern of the Piper for the flights 1, 7 and

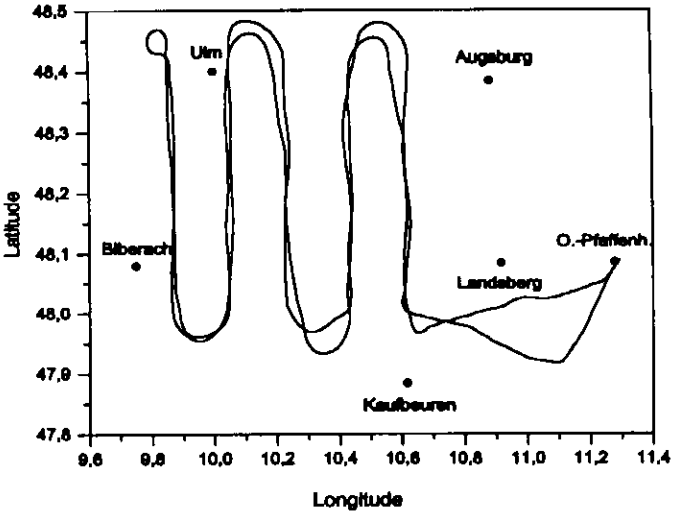

Figure 1a Flight plot from 25.5.92, Pattern C.

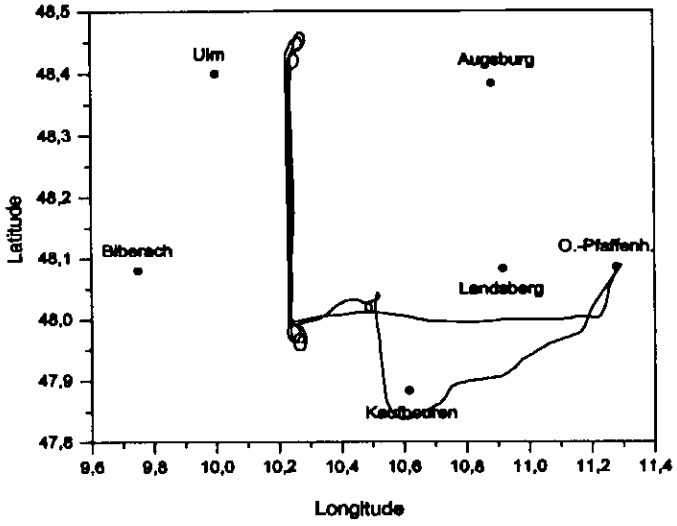

Figure 1b Flight plot from 25.7.92, Pattern A.

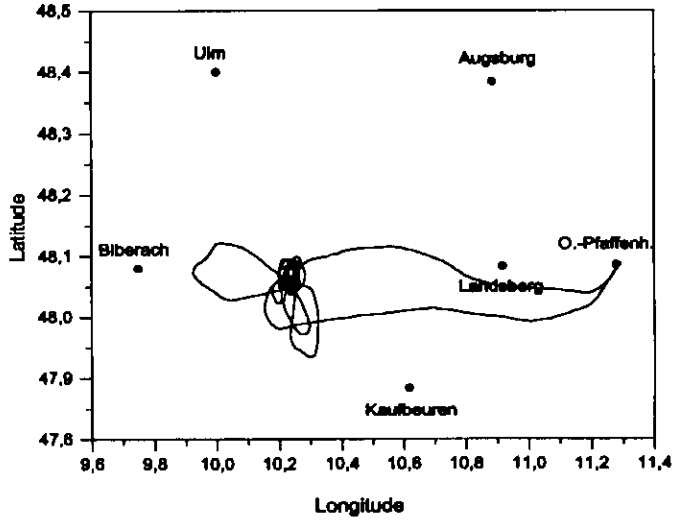

Figure 1c Flight plot from 1.6.92, single cumulus.

Table 1 CLEOPATRA flights and flight pattern. The flight pattern are named according to figure 1. s-Cu means that measurements were done in a single cumulus cloud, Cb indicates a thunder cloud.

	CLEOPATRA I					CLEOPATRA II	
Flight No.	1	2	3	4	5	6	7
Date	21.05	25.05	01.06	02.06	03.06	22.07	25.07
Pattern	C	C	s-Cu	Cb	B	B	A

3 can be seen as an example. The position of the aircraft was indicted and recorded during the flight by the aid of a global positioning system (GPS).

3 Results and Discussion

During the CLEOPATRA campaign seven measuring flights were carried out. All flights are listed in Table 1 together with the conducted flight pattern. Two of these flights were done according to pattern C (Figure 1) in nearly cloud free atmosphere with scattered cumulus convection while for three flights pattern A and B were chosen due to a stratiform cloud cover. Two flights were done in single cumulus clouds. During the flights no. 3 to 7 cloud water samples have been collected. Some of the measured data are discussed in the following section. It is differentiated between flights with low cloud cover (case 1) and flights with overcasted sky (case 2). Results of the gasphase measurements are presented for both aircraft whereas the shown data for the cloud water analysis are sampled by the Piper.

3.1 Measurements in the Gasphase

Case 1

At the beginning of the campaign two flights were performed according to pattern C. The Piper was measuring at a height of about 1000 m above ground, the DO-228 at a height of about 2500 m above ground. In a nearly cloud free atmosphere concentrations of the trace gases O_3, NO, NO_2, NO_x, H_2O_2 and SO_2 were measured. The nitrogen compounds were only measured at the DO-228, whereas the peroxide was measured at the Piper. As an example the concentrations measured during flight 1 (21th of May, afternoon) are plotted versus time in Figure 2a–2e. All concentrations are given in parts per billion by volume of air (ppbv). The H_2O_2 data collected with the Piper show values up to 1.5

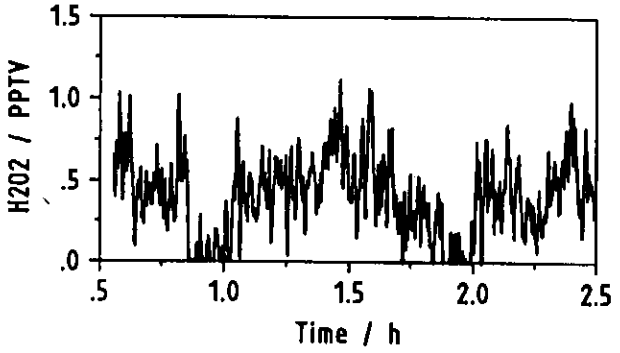

Figure 2a Temporal variation of the H_2O_2 concentration during flight 1 (concentration in ppbv).

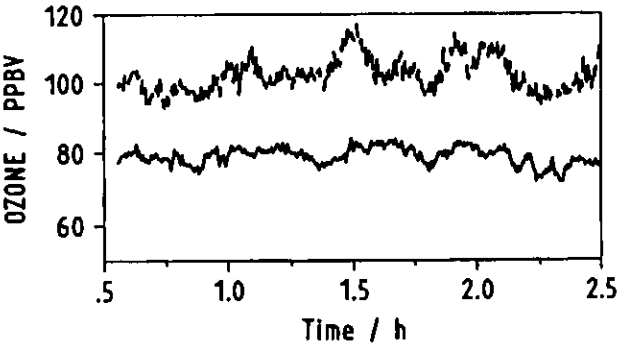

Figure 2b Temporal variation of the O_3 concentration during flight 1 (concentration in ppbv). The full line represents data collected at the Piper, the dashed line corresponds to data collected at the DO-228.

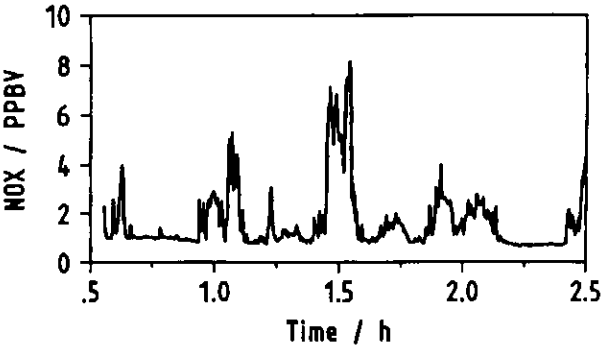

Figure 2c Temporal variation of the NO_x concentration during flight 1 (concentration in ppbv).

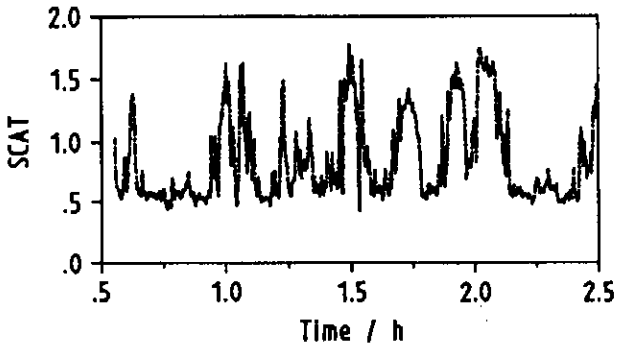

Figure 2d Temporal variation of the scattering coefficient during flight 1.

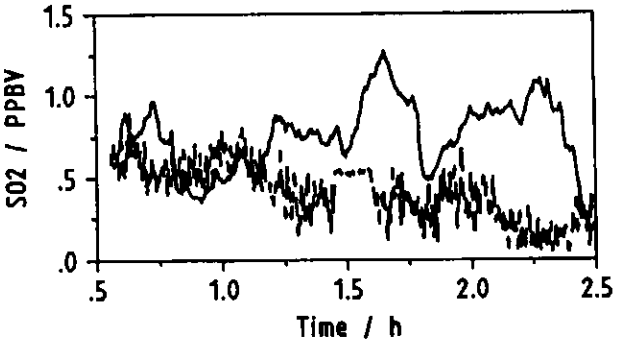

Figure 2e Temporal variation of the SO_2 concentration during flight 1 (concentration in ppbv). The full line represents data collected at the Piper, the dashed line corresponds to data collected at the DO-228.

ppbv (Figure 2a). In Figure 2b the ozone concentration at the two flight levels is shown. At the lower height ozone reaches mean values of about 80 ppbv, the ozone concentration at the height 2500 m above ground are about 25 ppbv higher. These measurements are in correspondence with vertical background ozone profiles. The ozone peaks in the two curves are correlated and also correlated with the peaks in the NO_x time series (Figure 2c). As scan be seen from Figure 2d showing the scattering coefficient, which indicates the occurrence of cloud, higher concentrations of O_3 and also NO_x had been observed within the cloud. This result was found for all measurements in small cumulus clouds. Especially for the presented data of flight 1 the mean ozone value in clouds was about 6 ppbv higher than in cloud free atmosphere. Laboratory tests showed, that the ozone detector is not sensitive to the humidity. Therefore the quality of the obtained ozone data is guaranteed. Big cumulus and stratocumulus clouds reduce the gaseous concentrations of O_3, NO_x and HO_2. HO_2 is rapidly scavenged by the droplets and dissociates (Lelieveld and Crutzen, 1991):

$$HO_2 = O_2^- + H^+ \quad (1)$$

Ozone is then destroyed by O_2^- via:

$$O_3 + O_2^- + H_2O = OH + 2O_2 + OH^- \quad (2)$$

Furthermore the reaction under cloudless condition between HO_2 and NO, which leads to the formation of NO_2 and hence of O_3 is suppressed in clouds. NO and HO_2 are largely separated in clouds because in contrast to HO_2 NO dissolves very poorly. This chemical behaviour might not be valid in small cumulus clouds. Temperature and liquid water content (LWC) are the controlling factors of the solubility of gases, low temperatures and high LWC are increasing the solubility. In small cumulus clouds the soluble gases remain in the gaseous phase and therefore O_3 is not destroyed. The reason for the observed enhanced concentrations in small clouds is more dynamically. The convective transport of more polluted air masses from the surface into higher levels might cause an increase of trace gases in the gaseous phase in clouds. The SO_2 concentrations were very low (0–1 ppbv) and often below the detection limit of the analyser. Slightly higher values were found at the lower level (Figure 2e).

Case 2

Flights 3–7 took place under more cloudy conditions, especially during the flights 5 to 7 stratiform clouds were prevailing. In this section we present measurements collected on the Piper for the flight no. 5, which took place at the 3th of June 1992. We were measuring along pattern B in four different flight levels (6000, 7000, 8000 and 4000 ft). As an example of the interaction of cloud droplets with trace gases the temporal variation of the O_3 concentration is shown in Figure 3. These data are sampled at different heights and the measurements are not corrected with the vertical distribution of the background ozone (Figure 4). Nevertheless the influence of clouds on the ozone values can be seen. Clouds are indicated by the liquid water content which was measured by the heated-wire instrument. The ozone concentration in the gasphase is decreasing within the cloud. Thus the observed behaviour of ozone in the presence of clouds may be estimated as a confirmation of the theory of Lelieveld and Crutzen (1990,1991). However, also an increase of O_3 within clouds is observed. This behaviour occurred probably under more convective character of the stratiform cloud.

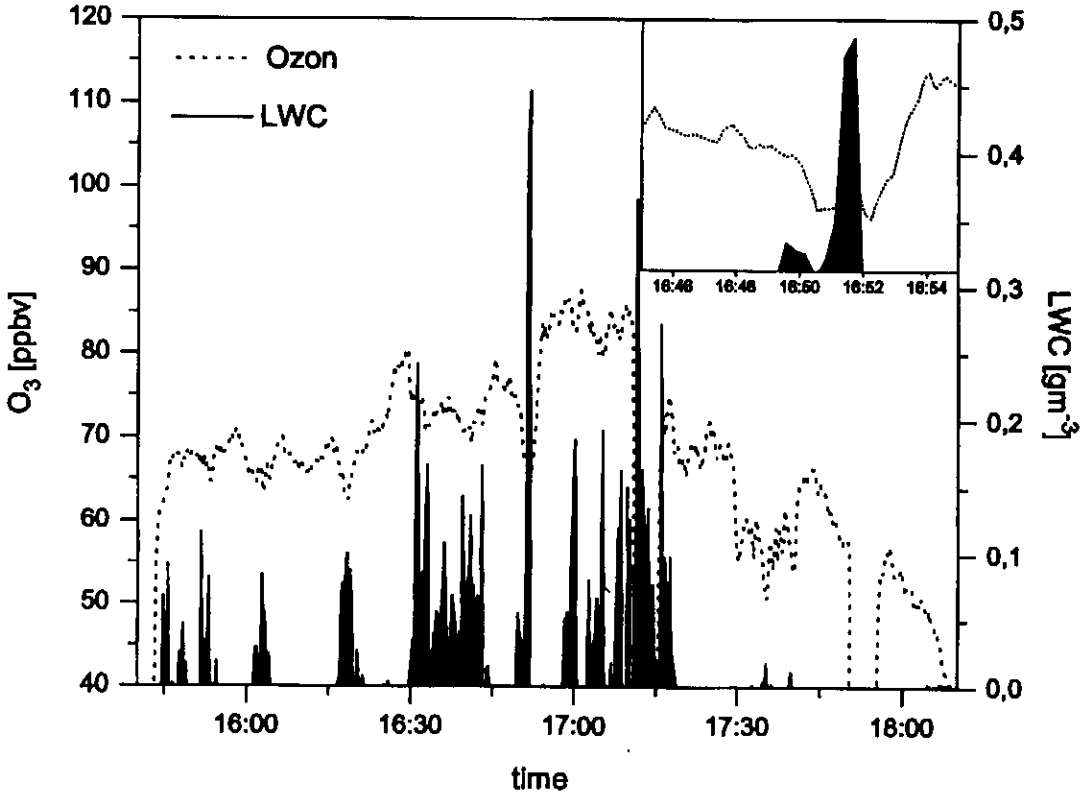

Figure 3 O_3 concentrations (in ppbv) in dependence of the liquid water content. The upper graphic shows a time period of ten minutes.

3.2 Cloud Water Analysis

During the experiment 53 cloud water samples have been collected. The results of the cloud water analysis are compiled in Table 2. The liquid phase equivalent air concentration was calculated from cloud water concentrations by the aid of cloud liquid water content:

$$c_{(air)}\,[\mathrm{nmol\,m^{-3}}] = c_{(cloud)}\,[\mu\mathrm{mol\,l^{-1}}] \times \mathrm{LWC}\,[\mathrm{ml\,m^{-3}}] \quad (3)$$

Some preliminary results should be discussed in more detail:

pH

pH and conductivity analyses have been carried out immediately after landing The pH during the first measuring period in May was unusually high, ranging between 5.4–6.9. The reason for this are obviously high NH_4^+ concentrations. During the second part of the campaign in July the pH varied in the range of 3.5 to 5.9.

Anions/Cations

Analysis of cloud water samples for inorganic cations $H^+, NH_4^+, Na^+, K^+, Ca^{2+}$ and Mg^{2+} established that in most samples the overwhelming fraction of equivalents was represented by NH_4^+. Similarly the anionic composition was dominated by SO_4^{2-} and NO_3^- while concentrations of Cl^- have generally been much lower. During flight 5 and flight 7 the concentrations of various ions were

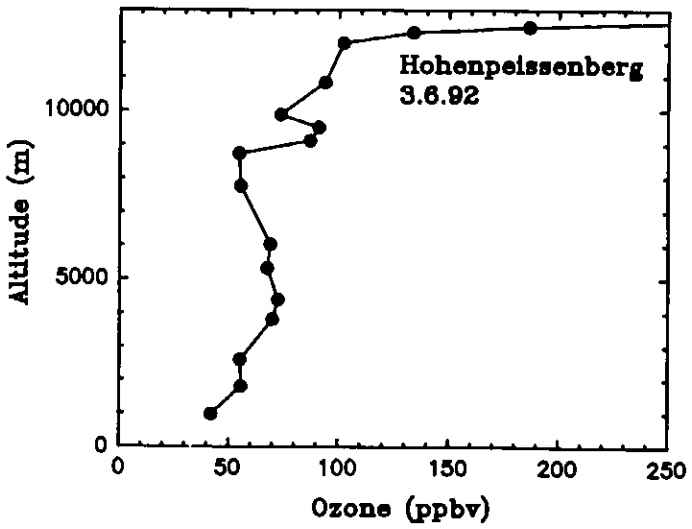

Figure 4 Vertical profile of the O_3 backgroundd concentration in ppbv. Radiosonde-data from Deutscher Wetterdienst Hohenpeissenberg.

Table 2 Cloud water analysis (concentration in neq/m^3). The sample were named according to Maser et al. (this issue). Cd. stands for conductivity measurements.

Flight	Code	Start	Stop	FL	pH	Cd. neq./ m^3	S(IV) neq./ m^3	H_2O_2 neq./ m^3	SO_4^{2-} neq./ m^3	NO_3^- neq./ m^3	Cl^- neq./ m^3	Na^+ neq./ m^3	K^+ neq./ m^3	NH_4^+ neq./ m^3	Mg^{2+} neq./ m^3	Ca^{2+} neq./ m^3
3	ICPS1	16 40	17 27	95	–	–	0.20	4.33	8.36	8.36	–	1.29	2.66	22.04	6.38	6.38
	ICPSn1	16 42	17 24	95	–	–	0.22	–	–	–	–	–	–	–	–	–
	K1	16 40	17 15	95	–	–	0.27	–	32.66	26.13	–	8.09	30.81	14.63	9.94	22.58
	K2	17 15	17 24	95	–	–	0.21	6.16	10.30	10.00	–	3.54	8.38	18.79	5.25	7.27
	K3	17 24	17 27	95	–	–	0.12	–	–	–	–	–	–	–	–	–
	M1	16 40	17 27	95	–	–	0.13	4.33	6.54	6.00	–	1.29	1.67	17.48	3.65	4.26
4	ICPS1	15 33	16 00	65	–	–	–	–	4.99	6.32	–	2.03	2.26	8.89	4.37	5.46
	ICPSn1	15 33	15 42	65	–	–	–	0.97	2.27	1.84	–	2.21	1.13	3.62	2.48	2.81
	ICPSn2	15 48	16 00	65	–	–	–	2.83	7.47	6.36	–	3.84	2.22	7.68	4.85	5.25
	ICPSn4	16 00	16 16	75	6.77	21	–	0.74	2.85	2.58	4.23	3.08	1.56	5.38	2.22	2.48
	ICPSN5	16 16	16 35	85	–	–	–	0.02	0.10	0.13	–	0.03	0.02	0.14	0.07	0.11
	K1	15 33	15 42	65	9.13	108	–	0.92	5.94	6.75	5.45	7.51	2.86	4.32	21.17	62.21
	K2	15 42	15 55	65	9.32	47	–	1.39	4.92	4.07	–	2.57	1.82	8.24	8.13	43.87
	K3	15 55	15 57	65	–	–	–	1.76	5.15	6.79	–	2.81	1.99	9.01	7.72	57.56
	M1	15 33	15 42	65	6.82	15	–	0.65	2.48	2.32	–	1.30	0.97	3.89	2.48	3.02
	M2	15 42	16 00	65	6.75	24	–	1.09	4.73	5.10	–	2.00	1.55	9.28	4.73	5.64
5	ICPSN1	15 49	16 24	60	–	–	0.01	–	14.40	21.12	1.56	1.22	0.65	1.39	–	–
	ICPSn2	16 28	16 49	870	–	–	–	11.16	34.92	74.50	9.02	3.69	3.59	73.72	6.98	14.94
	ICPSn4	16 54	17 17	100	–	–	–	14.69	29.55	24.92	6.68	7.48	2.76	35.24	10.15	37.91
	ICPSn5	17 17	17 24	100	–	–	–	–	–	–	–	2.06	1.08	18.45	2.92	6.02
	K1	15 49	15 59	60	–	–	–	–	32.97	0.77	1.54	1.51	1.37	2.91	4.83	9.17
	K2	15 59	16 24	60	–	–	–	–	18.02	4.41	1.26	1.20	1.05	8.80	3.40	12.39
	K3	16 28	16 36	70	–	–	0.04	3.61	58.50	24.72	4.84	7.62	3.50	42.75	10.51	33.17
	K4	16 36	16 49	70	5.42	68	0.01	10.67	14.54	15.73	1.93	2.21	1.93	36.62	4.42	4.60
	K5	16 49	16 54	70	–	–	0.11	13.40	20.09	24.82	4.14	5.91	3.55	46.10	10.24	10.64
	K6	16 54	17 02	100	–	–	0.03	–	5.85	8.50	–	2.58	1.22	12.78	3.40	3.26
	K7	17 02	17 17	100	5.54	37	0.04	12.73	10.71	10.30	2.42	3.13	1.92	15.76	5.25	2.02
	K8	17 17	17 24	100	–	–	0.01	5.89	4.56	4.52	–	1.16	0.69	6.84	2.24	1.29
	M1	15 49	16 49	60	–	–	–	–	2.74	3.71	–	1.40	0.84	13.37	1.06	2.35
	M3	16 54	17 17	100	–	–	0.04	10.89	13.32	14.76	–	3.87	1.71	16.74	6.84	12.78
6	ICPSn1	11 47	12 09	60	–	–	0.04	1.41	6.69	3.95	–	1.29	0.76	14.33	–	1.14
	ICPSn2	12 13	12 34	80	–	–	–	–	2.46	1.71	–	1.46	0.56	4.34	–	–
	ICPSn3	12 38	12 56	100	–	–	–	–	0.48	–	–	–	–	–	–	–
	ICPSn4	12 59	13 20	120	–	–	–	–	13.26	7.33	–	1.33	0.82	15.05	0.78	3.82
	K1	11 47	11 56	60	5.89	120	0.07	1.33	8.34	3.23	–	3.31	1.51	4.47	2.32	5.16
	K2	11 56	12 09	60	4.67	33	–	–	4.69	2.45	–	0.84	0.42	6.13	0.28	1.33
	K3	12 13	12 23	80	–	–	0.03	1.15	2.83	1.80	–	0.34	0.24	4.66	0.19	0.86

Table 2 (continued)

Flight	Code	Start	Stop	FL	pH	Cd. neq./ m^3	S(IV) neq./ m^3	H_2O_2 neq./ m^3	SO_4^{2-} neq./ m^3	NO_3^- neq./ m^3	Cl^- neq./ m^3	Na^+ neq./ m^3	K^+ neq./ m^3	NH_4^+ neq./ m^3	Mg^{2+} neq./ m^3	Ca^{2+} neq./ m^3
	K4	12 23	12 34	80	–	–	–	–	5.46	3.29	0.78	0.40	0.37	5.86	0.43	1.86
	K5	12 38	12 46	100	3.68	73	0.01	0.37	3.00	1.78	0.02	0.42	0.22	2.76	–	–
	K6	12 46	12 56	100	3.80	77	–	–	3.65	2.26	0.02	–	–	–	–	–
	K7	12 59	13 09	120	3.55	81	0.03	2.28	7.98	5.01	0.11	0.77	0.49	7.21	0.56	2.52
	K8	13 09	13 20	120	3.51	98	–	–	9.81	5.90	0.23	0.50	0.32	10.35	0.54	2.07
	M1	11 47	12 09	60	–	–	0.04	1.37	4.86	3.38	1.25	0.27	0.30	0.72	–	–
	M2	12 13	12 34	80	–	–	–	–	3.30	1.71	–	–	–	–	–	–
	M3	12 38	12 56	100	–	–	–	–	3.28	1.71	–	–	–	–	–	–
	M4	12 59	13 20	120	–	–	0.05	5.42	11.70	7.72	–	0.62	0.43	10.37	0.70	2.57
	N1	11 47	12 09	60	–	–	0.04	0.76	3.80	2.70	1.33	1.75	1.52	3.15	0.91	1.60
	N2	12 13	12 34	80	–	–	–	–	1.29	1.99	2.27	1.04	2.13	0.70	0.22	0.78
	N3	12 38	12 56	100	–	–	–	–	2.49	1.47	0.41	0.99	0.66	2.52	–	–
	N4	12 59	13 20	120	4.14	66	0.05	2.65	9.52	5.89	0.20	1.48	1.64	8.35	1.17	2.89
7	K1	10 59	11 22	60	4.06	72	0.01	0.22	2.18	2.82	–	0.96	0.44	11.63	–	–
	K2	11 28	11 51	100	3.81	81	0.02	1.30	5.15	–	–	0.53	0.70	7.40	0.55	2.30
	M2	11 28	11 51	100	–	–	0.02	2.43	6.00	6.85	–	–	–	–	0.40	1.55

measured in dependence of the flight height. In Figure 5 the ion concentrations versus the flight height is depicted. The two profiles are showing remarkable differences. While at 3th of June 1992 the highest ion concentrations were found in the level of 7000 ft the highest concentrations at 22th of July 1992 were found in the upper flight level at 12000 ft. Highest variations of ion concentrations were found for SO_4^{2-}, NO_3^-, NH_4^+ and H^+. This leads to the conclusion that these ions originate from chemical reactions.

H_2O_2

The H_2O_2 cloud water concentrations have been determined immediately after sampling on board of the aircraft. Due to rapid reaction of H_2O_2 with S(IV) a direct analysis is necessary for the correct determination of H_2O_2. The obtained concentration values between 10 to 155 $\mu mol l^{-1}$ are relatively high compared to measurements conducted previously between May–September 1986 over the North See (Franke and Jaeschke, 1993). At that time concentrations between 2 and 17 µmol/l were measured with a maximum in August.

S(IV) and HAS

The concentrations of S(IV) ranged between 0.1 and 4.0 $\mu mol l^{-1}$. Concentrations of hydroxyalkylsulfonats (HAS) were also measured. With concentrations between 0.3 and 2.0 µmol/l they represent an amount of 50–70 % of total S(IV). In contrast during a flight conducted in July 1992 over the northern part of Germany only 20 % of HAS could be found. As can be seen in Table 2, H_2O_2 concentrations are always in high excess compared to S(IV) concentrations. This is a hint that S(IV) is continuously consumed by H_2O_2, while HAS is stable against it's attack. Therefore it can be concluded that the amount of HAS in total S(IV) was relatively high during the CLEOPATRA experiment.

Reactions of S(IV) with H_2O_2

Some of the cloudwater samples, which had been analysed for S(IV) and H_2O_2 during the flights were analysed for a second time after landing. Time periods between these two determinations lasted up to 4 h. After this long period it was expected that S(IV) is no longer existent in samples with high H_2O_2 concentrations. However, the second analysis

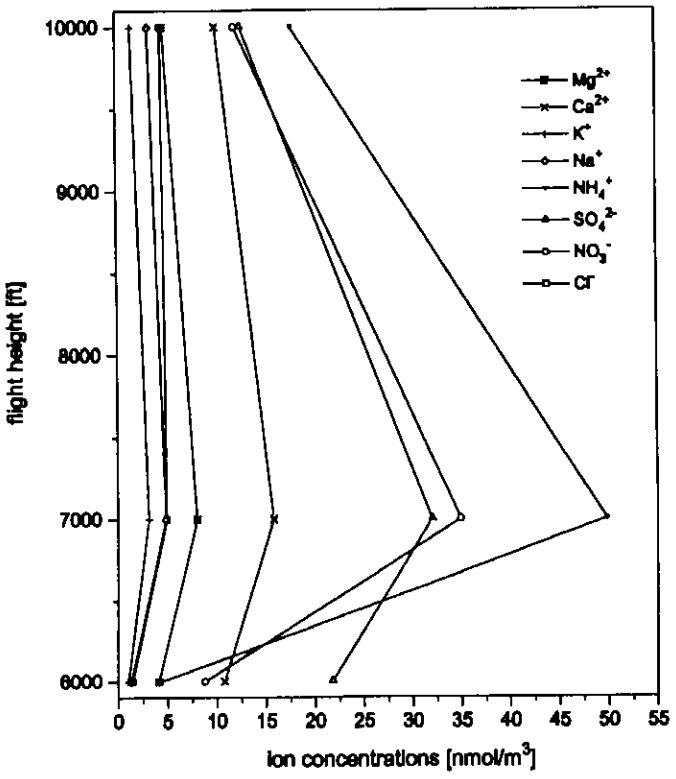

Figure 5a Concentrations of major anions and cations (in $nmol/m^3$) in dependence of the flight height at 3.6.92.

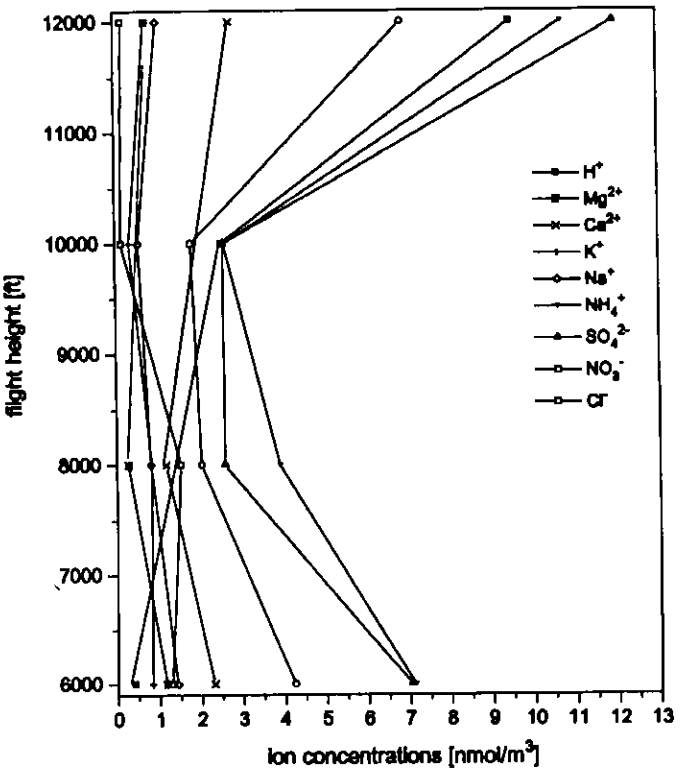

Figure 5b Concentrations of major anions and cations (in $nmol/m^3$) in dependence of the flight height at 22.7.92.

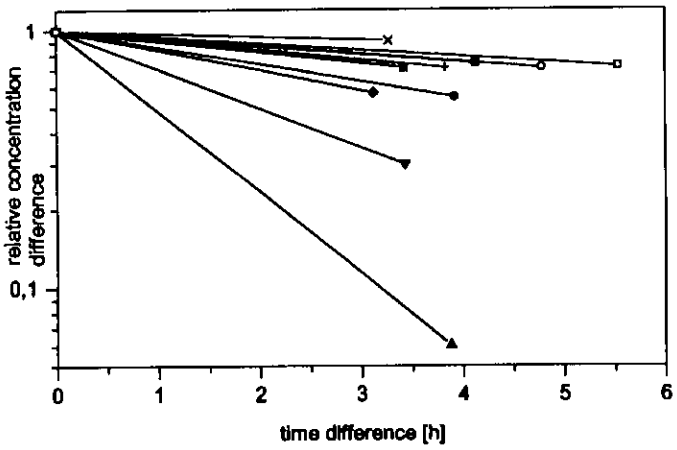

Figure 6 The decay rate of S(IV) in cloud water samples. The concentration measured on board of the aircraft was normalised to one.

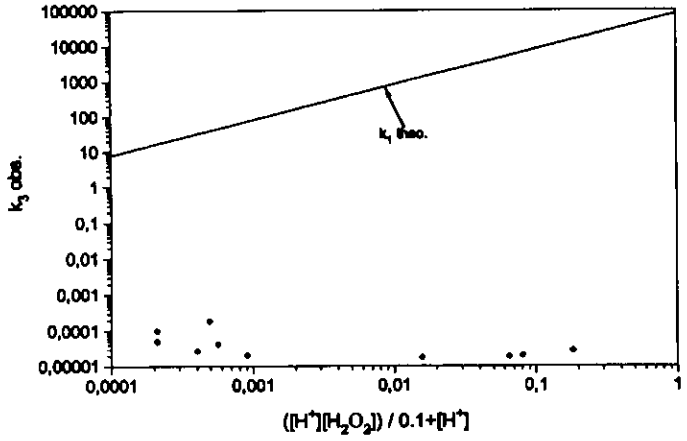

Figure 7 The observed rate constant k_3 is plotted against the quotient $([H^+]\,[H_2O_2])/0.1 + [H^+]$. The straight line shows the theoretical slope k_1 according to Eq. (4).

performed at ground showed significant S(IV) concentrations even in samples with high H_2O_2 excess. Figure 6 shows the decay rate of S(IV) observed in the samples. It can be seen in Figure 6 that the decay rate of S(IV) varies in each sample. Martin and Damschen (1981) proposed the following rate equation for the reaction of S(IV) with H_2O_2:

$$-dS(IV)/dt = (k_1 \times [H_2O_2] \times [H^+] \times [HSO_3^-])/0.1 + [H^+] \quad (4)$$

Since the $[H^+]$ and $[H_2O_2]$ are high in comparison to the $[HSO_3^-]$ they are considered as a constant and included in a rate coefficient k_3. Eq. (4) can be summarised to Eq. (5):

$$-d\,[HSO_3^-]/dt = k_3\,[HSO_3^-] \quad (5)$$

The rate coefficients k_3 were calculated from our experimental data set and plotted against the quotient $([H^+]\,[H_2O_2]/0.1 + [H^+])$. The result can

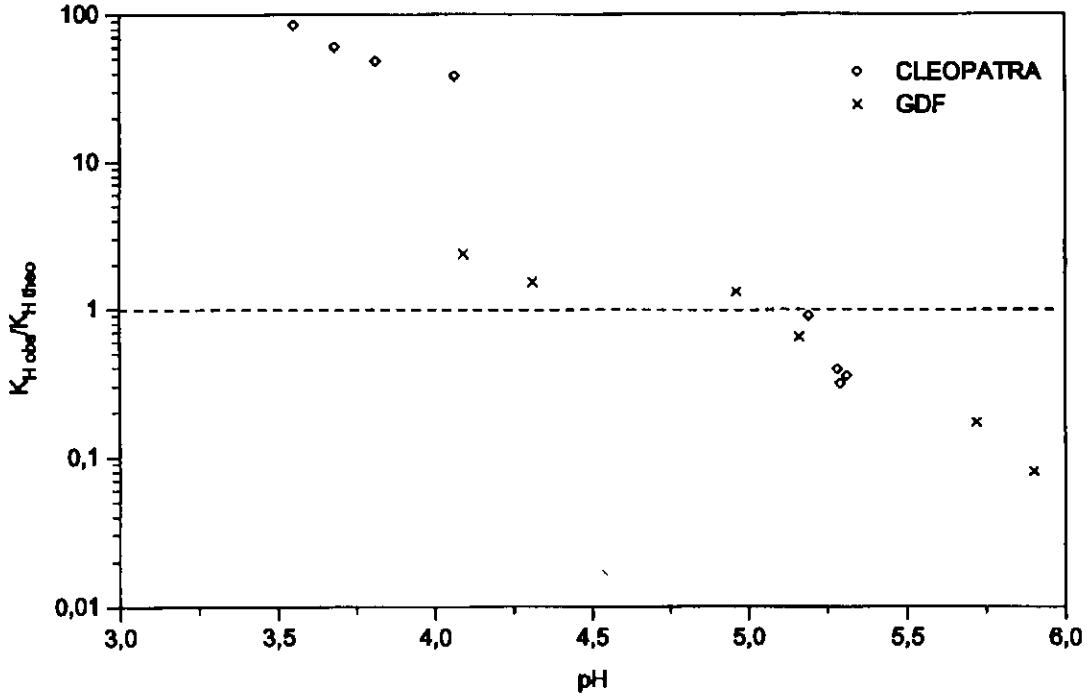

Figure 8 Deviations from Henry's law equilibrium for S(IV). Data from a experiment at Great Dun Fell (GDF) are included.

be seen in Figure 7. Theoretically the result should be a straight line with the slope k_1 (see Eq. (4)). As can be seen in Figure 7 k_3 is not at all correlated linearly with $[H_2O_2]$ and $[H^+]$. Furthermore the values are much lower than theory predicts. This means that the reaction in the collected samples is much slower than we expected. Since no obvious trend can be seen in Figure 7, no hint on the nature of this coexistence of S(IV) and H_2O_2 is given. A stabilization of S(IV) in the samples due to complexation with formaldehyde can be excluded, since only free S(IV) has been measured. Detailed explanations of this phenomenon requires more extended data sets and will be subject of our further research.

Phase Partitioning

The gas/liquid partitioning of a given species is defined by its Henry's law constant K_H. In particular the distribution of S(IV) between the gas and aqueous phase is strongly dependent on the droplet pH, since S(IV) undergoes rapid acid-base equilibria in solution. A pseudo-Henry's law constant K_H is therefore defined to include this effect (Schwartz, 1984):

$$K_H = K_H(1 + K_1/[H^+] + K_1K_2/[H^+]^2) \quad (6)$$

where K_1 is the dissociation constant of the reaction

$$(SO_2)_{aq} = HSO_3^- + H^+ \quad (7)$$

and K_2 is the dissociation constant of the reaction

$$HSO_3^- = SO_3^{2-} + H^+ \quad (8)$$

The theoretical pseudo-Henrys law constant was calculated as a function of pH and compared with the experimental constant calculated from the gas and liquid phase measurements. Figure 8 shows the difference between the experimental and the theoretical Henry's law constant. Data from an experiment at Great Dun Fell in Great Britain are included. The plot is normalised in such a way that only discrepancies to Henry's law are shown. This means, the observed gas-to-liquid-ratio was divided by the theoretical pseudo-Henry's law constant at the specific pH. Numbers larger than unity indicate supersaturation of the liquid phase while smaller numbers indicate subsaturation of the liquid phase. Figure 8 shows that in dependence of the pH super- and subsaturation of the liquid phase up to a factor 20 can occure. In the literature deviations from Henry's law equilibrium are reported for different substances like organic acids and ammonia (Facchini et al., 1992; Winiwater et al., 1994). The following explanations have been discussed:

1. The complex formation of S(IV) with aldehydes shifts the phase equilibrium towards the liquid side (Munger et al., 1983; Joos and Baltensberger, 1991). Since we measure free S(IV) and HAS in different channels, we can exclude an overestimation of the liquid phase due to complex formation.
2. Pandis and Seinfeld (1992) reported that the mixture of droplets with different pH of which each is in Henry's law equilibrium with the surrounding atmosphere always results in a bulk cloud water sample that is supersaturated. Winiwater (1992) calculated that this effect can solely explain deviations up to a factor of 3. Therefore not all deviations observed during the CLEOPATRA experiment can be explained by the theory of Pandis and Seinfeld because with respect to the Henry's law equilibrium super- and subsaturation were observed and the supersaturations were often much larger than a factor of 3.
3. Winiwater et al. (1992) argued that the high variability of LWC in clouds can account for an undersaturation effect of bulk cloud water samples up to a factor of 20. Nonetheless this effect cannot entirely account for the large departures from Henry's law equilibrium observed in our samples.
4. The hypothesis has been reported in the literature (Gill et al., 1983) that organic films of surface active substances on cloud droplets would considerably reduce the mass exchange across the air/droplet interface. The organic film would produce the largest deviations from Henry's law equilibrium in the pH region where a higher mass transfer across the air/liquid interface is expected. However, organic films only explain subsaturation of the liquid phase.

None of these hypothesis can completely explain the observed deviations from the Henry's law equilibrium. Since Henry's law is assumed to be fulfilled in many modelling studies, the phase equilibrium under atmospheric conditions has to be an important field of further studies.

4 Conclusion

Some preliminary results of the CLEOPATRA field campaign have been presented. Seven measuring flights have been carried out and altogether 53 cloudwater samples have been analysed. At the first two flights the gasphase concentrations of trace gases in small cumulus clouds were observed. Due to dynamic effects the ozone concentration as well as the NO_x concentration is increasing within small clouds. According to the theory ozone is decreasing in more stratiform clouds. The analysis of cloud water samples showed that in contrast to previous studies (Daum et al., 1984) the pH of the cloud water is no longer acidic. During the measuring period cloud water samples with high pH up to neutrality have been collected. This high pH can be explained by high NH_4^+ concentrations and also by very low SO_2 concentrations. Due to these low SO_2 concentrations only little sulphate production can occur in the aqueous phase even if the oxidation potential of the aqueous phase is high.

Furthermore the phase equilibrium of S(IV) has been studied. In dependence of the pH super- as well as subsaturation of the liquid phase with respect to Henry's law has been measured. Since Henry's law is applied in many studies a detailed examination of the phase equilibrium has to be subject of further research.

References

Daum, P. H., T. J. Kelly, S. E. Schwartz and *L. Newman,* 1984: Measurements of the chemical composition of stratiform clouds. Atmos. Environ. **18,** 2671–2684.

Facchini, M. C., S. Fuzzi, J. A. Lind, H. Fierlinger-Oberlinninger, M. Kalina, H. Puxbaum, W. Winiwarter, B. G. Arends, W. Wobrock, W. Jaeschke, A. Berner and *C. Kruisz,* 1992: Phase-partitioning and chemical reactions of low molecular weight organic compounds in fog. Tellus **44B,** 533–544.

Gill, P. S., T. E. Graedel and *C. J. Weschler,* 1983: Organic films on atmospheric particles, fog droplets, cloud droplets, raindrops and snowflakes. Rev. Geophys. Space Phys. **21,** 903–920.

Jaeschke, W. and *H. Franke,* 1992: H_2O_2 in cloud and fog water. The proceedings of EUROTRAC symposium '92 edited by P. M. Borrell et al., 486–489.

Joos, F. and *U. Baltensperger,* 1991: A field study on chemistry, S(IV) oxidation rates and vertical transport during fog conditions. Atmos. Environ. **25A,** 217–230.

Lelieveld, J. and *P. J. Crutzen,* 1990: Influences of cloud photochemical processes on tropospheric ozon. Nature **343,** 227–233.

Lelieveld, J. and *P. J. Crutzen,* 1991: Influences of cloud in trophospheric photochemistry. J. Atmos. Chem. **12,** 229–267.

Martin, R. and *D. E. Damschen,* 1981: Aqueous oxidation of SO_2 by H_2O_2 at low pH. Atmos. Environ. **15,** 1615–1621.

Maser, R., H. Franke, M. Preiß and *J. Jaeschke,* 1994: Methods provided and applied in a small research aircraft for the study of cloud physics and chemistry. Contr. Atmos. Phys. **67,** 321–334.

Mohnen, V., F. Cosmeier and *F. Fiedler,* 1992: EUROTRAC subproject TRACT: Quality assurance project plan aircraft measurement systems. TRACT report, EUROTRAC office. Fraunhofer Institut für atmosphärische Umweltforschung, Garmisch-Partenkirchen, 184 pp.

Munger, J. W., D. J. Jacob, J. M. Waldman and *M. R. Hoffmann,* 1983: Fogwater chemistry in an urban atmosphere. J. Geophys. Res. **88,** 5109–5121.

Pandis, S. N. and *J. H. Seinfeld,* 1991: Should bulk cloud water or fog water samples obey Henr's law? J. Geophys. Res. **96,** 10791–10798.

Schwarzt, S. E., 1984: in: Calvert, J. G. (ed.), SO_2, NO and NO_2 oxidation mechanisms: Atmospheric considerations. Butterworth, Boston, 173.

Winiwarter, W., B. Brantner and *H. Puxbaum,* 1992: Comment on "Should bulk cloud water or fog water samples obey Henry's law?" by S. N. Pandis and J. H. Seinfeld. J. Geophys. Res. **97,** 6075–6078.

Winiwarter, W., H. Fierlinger, H. Puxbaum, M. C. Facchini, B. G. Arends, S. Fuzzi, D. Schell, U. Kaminski, S. Pahl, T. Schneider, A. Berner, I. Solly and *C. Kruisz,* 1994: Henrys law and the behavior of weak acids and bases in fog and cloud. J. Atmos. Chem., in press.